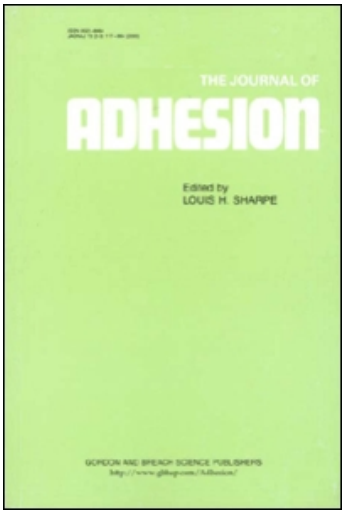

The Journal of Adhesion
Publication details, including instructions for authors and subscription information:
http://www.informaworld.com/smpp/title~content=t713453635

Macroscopic Behavior of Carbon Nanotube (CNT)-Reinforced Composite Accounting for Interface Cohesive Force

L. Y. Jiang[a]
[a] Department of Mechanical and Materials Engineering, The University of Western Ontario, London, ON, Canada

Online publication date: 12 March 2010

To cite this Article Jiang, L. Y.(2010) 'Macroscopic Behavior of Carbon Nanotube (CNT)-Reinforced Composite Accounting for Interface Cohesive Force', The Journal of Adhesion, 86: 3, 273 — 289
To link to this Article: DOI: 10.1080/00218460903466633
URL: http://dx.doi.org/10.1080/00218460903466633

The Journal of Adhesion, 86:273–289, 2010

ISSN: 0021-8464 print/1545-5823 online
DOI: 10.1080/00218460903466633

Taylor & Francis
Taylor & Francis Group

Macroscopic Behavior of Carbon Nanotube (CNT)-Reinforced Composite Accounting for Interface Cohesive Force

L. Y. Jiang
Department of Mechanical and Materials Engineering,
The University of Western Ontario, London, ON, Canada

The large aspect ratio of interfacial area per unit volume at CNT/matrix interfaces may significantly influence the macroscopic behavior of CNT-reinforced composites. The property of interfaces is governed by the cohesive law, which is determined from both van der Waals forces and chemical covalent bonds. This nonlinear cohesive law is incorporated in the micromechanics model in the current work to study the mechanical behavior of CNT-reinforced composites. It is found that carbon nanotubes can improve the macroscopic behavior of the composite at small strain, but tend to weaken the composite at relatively large strain because of the interface softening behavior or debonding. The increase of interface adhesion caused by the creation of chemical covalent bonds may significantly improve the composite behavior at large strain.

Keywords: Carbon nanotubes (CNTs); Chemical bond; Interfacial cohesive law; Nanocomposite; van der Waals force

INTRODUCTION

Since the discovery of carbon nanotubes (CNTs) by Iijima [1], these novel materials have triggered extensive research interests in their properties. Existing studies have shown that the Young's modulus of CNTs is on the order of 1 TPa [2–5] and their tensile strength is extraordinarily high [6–8]. These superior mechanical properties make

Received 13 July 2009; in final form 16 September 2009.
Presented in part at the 3rd Canadian Conference on Nonlinear Solid Mechanics (CanCNSM 2008), 25–29 June 2008, Toronto, Ontario, Canada.
Address correspondence to L. Y. Jiang, Department of Mechanical and Materials Engineering, The University of Western Ontario, London, ON N6A 5B9, Canada. E-mail: lyjiang@eng.uwo.ca

CNTs very promising candidates as ideal reinforcements for nanocomposites [9–13]. However, recent studies on the performance of CNT composites reported both encouraging results and moderate improvements of CNTs in the polymer matrix [14–18]. The discrepancy of the mechanical properties of CNT composites from expectation needs further investigation.

Since the CNT-reinforced composites in general possess a large amount of interfaces due to the small size of carbon nanotubes, the interface behavior and the interfacial load transfer efficiency may significantly influence the macroscopic properties of composites. Some efforts have been made to assess the load transfer ability through the CNTs/matrix interface using experimental and atomic simulations [16,19–24] and continuum-based models [25–27]. These studies shed light on understanding the behavior of CNT/matrix interfaces, but do not provide a direct link between the CNT/matrix interface and the macroscopic properties of the nanocomposites.

It is difficult to incorporate the interface behavior directly into the continuum modeling of nanocomposite properties. Based on the van der Waals force only, Jiang *et al.* [28] established a nonlinear cohesive law for CNT/polyethylene matrix interfaces, in which the normal cohesive stress was derived directly in terms of the interface opening displacement. The properties of the interface cohesion, such as the cohesive strength and total cohesive energy, are expressed in terms of the parameters in the Lennard-Jones (LJ) potential, carbon atom area density for CNTs, and molecular volume density for the matrix. Such an approach from the basis of the atomic study avoids any assumed phenomenological cohesive laws, and accurately accounts for the van der Waals force in the continuum model. This nonlinear cohesive law has been incorporated in the micromechanics model by Tan *et al.* [29] to study the effect of the interface behavior upon the macroscopic properties of CNT-reinforced composites. Their study indicated that CNTs can indeed improve the mechanical behavior of a composite at small strain, but such improvement disappears at relatively large strain or may even weaken the composite. It is also found that the increase of interface adhesion between CNTs and polymer matrix may significantly improve the composite behavior at large strain.

The improvement of the adhesion between CNTs and polymer matrix may be realized by the creation of new chemical bonds at the interfaces. Frankland *et al.* [22] have predicted that the shear strength for the CNT/matrix interface can be enhanced by more than an order of magnitude with the artificial formation of cross-links involving less than 1% of the carbon atoms on the CNTs using molecular simulation.

It should be mentioned that the new interfacial chemical bonds are usually created through the functionalization of the surfaces of the CNTs [30–33] by introducing sp^3 hybridized sites for some carbon atoms on the CNT surface. Accounting for these chemical bonds at the CNT/matrix interfaces, Jiang [34] established a cohesive law for the opening deformation mode of the interfaces. In addition to the parameters [28] in the cohesive law, the material constants of the carbon nanotube and polymer matrix, the parameters in Brenner potential describing the chemical bond potential energy, and the chemical bond density all contribute to the interface adhesion.

The objective of this paper is to incorporate the nonlinear cohesive law [34] accounting for both van der Waals force and chemical bond effects at CNT/polyethylene matrix interfaces in the micromechanics study of CNT-reinforced composite behavior. It provides an assessment on how the improved interfacial adhesion influences the macroscopic properties of nanocomposites.

THE NONLINEAR COHESIVE LAW FOR INTERFACE OF CNT/MATRIX

For CNT composites, one of the major differences in behavior from the conventional composites is the fact that the interface of CNT/matrix has a much larger surface area per unit volume, *i.e.*, $S/V = \frac{2}{R_0}$ with R_0 being the nanotube radius. It is expected that interfaces may play a significant role in the macroscopic behavior of nanocomposites; therefore, it is essential to incorporating the interface effect *via* an interfacial cohesive law. Currently, we assume that the interface interaction is governed by both covalent chemical bonds and van der Waals forces. It has been verified by Jiang *et al.* [28] that the CNT radius effect upon the interfacial cohesive law is negligible. Thus, we neglect the effect of CNT radius and study the interaction between a graphene (*i.e.*, an infinite plane of carbon atoms) and polymer matrix to develop the interfacial cohesive law for simplicity. Figure 1 shows the deformation configuration of the system, in which the graphene is parallel to the polymer surface with h denoting their total normal separation distance. The graphene is a flat structure consisting of sp^2 hybridized carbon atoms with area density (number of carbon atoms per unit area of CNT) of $\rho_c = 3.82 \times 10^{19}\,\mathrm{m}^{-2}$, and the polymer matrix is assumed to be polyethylene (PE) with repeating $-CH_2-$ units of volume density (number of polymer molecules per unit volume) $\rho_p = 3.1 \times 10^{28}\,\mathrm{m}^{-3}$ [29]. The new chemical bond is assumed to form between a carbon atom, i, of graphene and a carbon atom, j, from the polyethylene matrix due to the depletion of a hydrogen atom

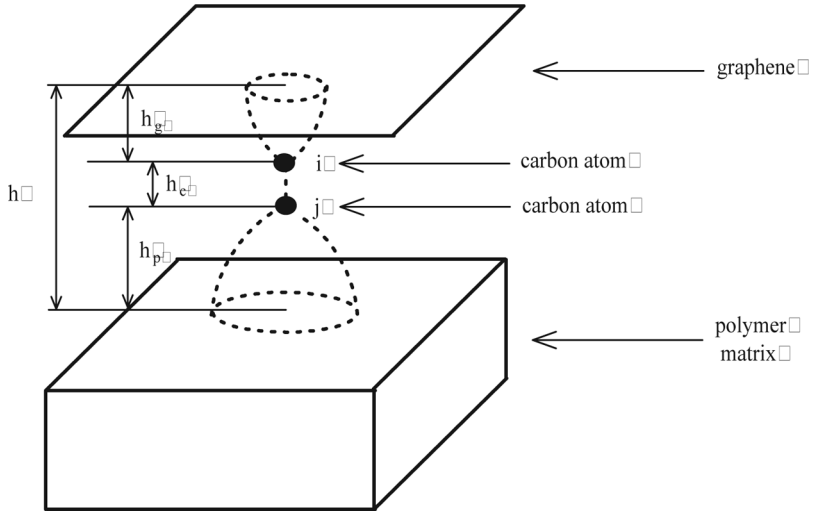

FIGURE 1 A schematic diagram of a graphene parallel to the surface of a polymer with a covalent carbon-carbon bond.

from the polymer chain, *i.e.*, the carbon atoms i and j stick out to form a new sp^3 C−C bond with bond length h_c. The formation of such new covalent C−C bonds between functionalized CNT and PE polymer matrix has been observed by Shofner *et al.* [33] through the Raman spectra of a composite sample containing fluorinated CNTs in the PE matrix. Mylvaganam and Zhang [31] also used quantum mechanics to predict that covalent bonding between an alkyl radical and a nanotube is energetically favorable. The density of carbon atoms involved in forming the covalent new bonds is assumed to be ρ. In this situation, the creation of a new sp^3 C−C bond is equivalent to applying force to each carbon atom, which can be determined from the chemical bond potential. This covalent bond force will cause the atom motion or the local deformation of both the graphene and the polymer matrix. The deformation of graphene around the atom i is modeled as a clamped circular plate with radius R_g subjected to a concentrated force (*i.e.*, the covalent force F), and the polymer matrix deformation around atom j is modeled as a half-infinite medium subjected to uniformly distributed force ($F/\pi {R_p}^2$) on a carbon atom with radius R_p. When the system is in equilibrium without applied external loading, the equilibrium separation distance between the graphene and polymer surface is $h = h_0$, and the covalent bond length is $h_c = h_{c0}$.

For the opening mode separation of the interface, *i.e.*, an opening displacement $[u_r]$ beyond the global equilibrium distance, h_0, which

is equivalent to a stretch of chemical bond length $[u_c]$ beyond h_{c0}, Jiang [34] established the following cohesive law for CNT/polymer interfaces:

$$\begin{aligned}\Phi_{cohesive}([u_r]) &= (1-\rho)\Phi_{vdW}([u_r]) + \rho\rho_c(\Phi_{ch}([u_r]) + \Phi_g([u_r]) + \Phi_P([u_r])) \\ &= (1-\rho)\Phi_{vdW}([u_c]) + \rho\rho_c(\Phi_{ch}([u_c]) + \Phi_g([u_c]) + \Phi_p([u_c]))\end{aligned} \tag{1}$$

$$\sigma^{\text{int}}([u_r]) = \frac{\partial\Phi_{cohesive}([u_r])}{\partial[u_r]} = \frac{\frac{\partial\Phi_{cohesvie}([u_c])}{\partial[u_c]}}{1 + \frac{\partial h_g([u_c])}{\partial[u_c]} + \frac{\partial h_p([u_c])}{\partial[u_c]}}. \tag{2}$$

The cohesive energy, $\Phi_{cohesive}$, in Eq. (1) is the energy stored per unit area consisting of four parts: the energy due to van der waals force, Φ_{vdW}; the energy due to covalent chemical bond, Φ_{ch}; and the strain energy of both graphene, Φ_g, and polymer matrix, Φ_p, which was discussed in detail by Jiang [34]. σ^{int} is the normal cohesive stress.

Based on the LJ 6–12 potential for van der Waals force, the cohesive energy Φ_{vdW} due to the van der Waals force was developed by Jiang *et al*. [28], as

$$\begin{aligned}\Phi_{vdW} &= \frac{2\pi}{3}\rho_p\rho_c\varepsilon\sigma^3\left(\frac{2\sigma^9}{15(h_0+[u_r])^9} - \frac{\sigma^3}{(h_0+[u_r])^3}\right) \\ &= \frac{2\pi}{3}\rho_p\rho_c\varepsilon\sigma^3\left(\frac{2\sigma^9}{15(h_{c0}+[u_c]+h_g([u_c])+h_p([u_c])^9}\right. \\ &\qquad \left. - \frac{\sigma^3}{(h_{c0}+[u_c]+h_g([u_c])+h_p([u_c]))^3}\right),\end{aligned} \tag{3}$$

where $\sqrt[6]{2}\sigma$ is the equilibrium distance between the atoms, ε is the bond energy at the equilibrium distance, and they take the values $\varepsilon = 0.004656\,\text{eV}$ and $\sigma = 0.3825\,\text{nm}$ for carbon atoms of the CNT and the $-\text{CH2}-$ units of polyethylene [23]. h_g and h_p are the maximum vertical displacements occurring at the center of the clamped plate and the center of the carbon atom forming the covalent bond in the polymer matrix.

The cohesive energy, Φ_{ch}, due to the covalent bond was determined from the second generation Brenner potential [35],

$$\begin{aligned}\Phi_{ch}([u_c])) &= (1 + \frac{Q}{(h_{c0}+[u_c])})Ae^{-\alpha(h_{c0}+[u_c])}f_c(h_{c0}+[u_c]) \\ &\quad - B_{ij}\sum_{n=1}^{3}B_n e^{-\beta_n(h_{c0}+[u_c])}f_c(h_{c0}+[u_c]),\end{aligned} \tag{4}$$

where B_{ij} is a bond order function and $f_c(h_{c0}+[u_c])$ is a continuous cutoff function. These functions and the other parameters in the above equation are given in [35] and discussed in detail by Jiang [34]. The change of covalent bond length $[u_c]$ results in a force acting on each individual carbon atom in the covalent bond, which is determined from the derivation of the potential energy, Φ_{ch},

$$F([u_c]) = -\frac{\partial \Phi_{ch}([u_c])}{\partial [u_c]}. \tag{5}$$

According to this covalent force and the assumed deformation models of graphene and polymer matrix as shown in Fig. 1, $h_g([u_c])$ and $h_p([u_c])$ in Eq. (3) are derived by Jiang [34] as

$$h_g([u_c]) = \frac{F([u_c])R_g^2}{8\pi D},\ h_p([u_c]) = \frac{(1-\nu_m^2)F([u_c])}{2\pi E_m R_p}, \tag{6}$$

where $D = 1.3787\,\text{eV}$ is the bending rigidity of graphene given in [36] from the interatomic potential, $E_m = 0.9\,\text{GPa}$ and $\nu = 0.33$ are Young's modulus and Poisson's ratio of polyethylene, respectively [23]. Meanwhile, the strain energies in the cohesive energy (1) for the graphene and polymer matrix are derived as

$$\Phi_g([u_c]) = \frac{F([u_c])^2 R_g^2}{16\pi D} \tag{7}$$

$$\Phi_p([u_c]) = \frac{8(1-\nu_m^2)F([u_c])^2 R_p}{3\pi^2 E_m}. \tag{8}$$

For the case when the covalent bond density $\rho = 0$, Eqs. (1) and (2) are reduced to the ones derived by Jiang *et al*. (28) considering van der Waals force only, in which the interface has a rather high cohesive strength ($\sigma_{\max}^{\text{int}} = 478\,MPa$) as compared with the Young's modulus of polyethylene ($\sim$0.9 GPa) but a very low cohesive energy ($\Phi_{cohesive}^{total} = 0.107\,Jm^{-2}$). When the covalent bonds are created, the poor bonding between CNTs and polymer matrix is expected to be improved. For different covalent bond densities, the normal cohesive stress for the interface *versus* interface opening displacement is plotted in Fig. 2 for comparison. Unlike the case considering van der Waals force only ($\rho = 0\%$), the interface demonstrates hardening behavior, then softening behavior and hardening behavior again due to the introduction of chemical bonds. The cohesive stress increases rapidly at small opening displacement, reaches the first maximum value at $[u_r]_{cr}^1$ (for example, $[u_r]_{cr}^1 = 0.0593\,nm$ for $\rho = 5\%$, which is very close to the critical separation distance for considering van der Waals force

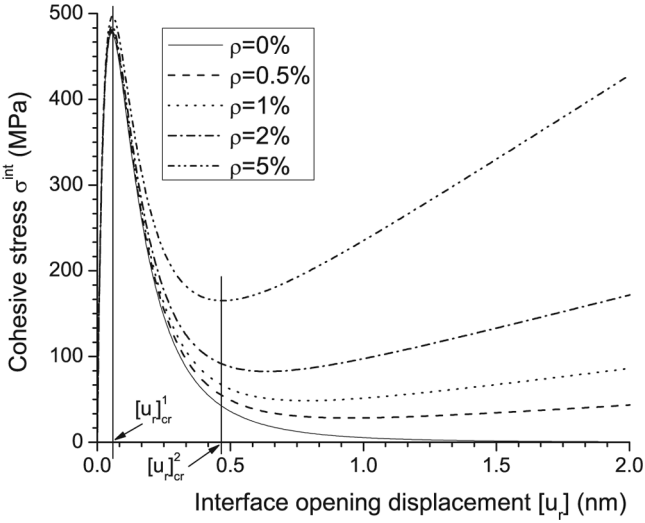

FIGURE 2 The cohesive law for CNT/polymer matrix interface established from van der Waals force and chemical bonds.

only, *i.e.*, 0.0524 nm [28]), and then gradually decreases as $[u_r]$ increases. This first hardening process is governed by both van der Waals force and covalent bonds, and the first maximum stress (479 MPa for $\rho = 0.5\%$, 481 MPa for $\rho = 1\%$, 485 MPa for $\rho = 2\%$, and 497 MPa for $\rho = 5\%$) increases slightly compared with the cohesive strength accounting for van der Waals force only (478 MPa $\rho = 0\%$). It should be mentioned that in this process, the van der Waals force plays a significant role as the first maximum stress and the critical interface separation are close for all these cases. However, this cohesive stress does not decay to zero in the softening process as in [28] when considering van der Waals force only (*i.e.*, $\rho = 0\%$). When $[u_r]$ reaches a special value $[u_r]^2_{cr}$ ($\rho = 5\%$ for example in the figure, which depends on the chemical bond density), the softening behavior is over with the increase of cohesive stress until the second maximum value when $[u_r]$ reaches its third critical separation $[u_r]^3_{cr}$ (which corresponds to the critical value for the covalent bond length, h_c^{cr}, associated with the maximum covalent bond force) as expected. After this point, the interface may experience the softening behavior again due to the decrease of covalent bond force. This second hardening process and beyond are not completely drawn in this figure since when this critical $[u_r]^3_{cr}$ is reached, the total interface separation is too large and may be far beyond where the polymer chain remains adhered to the rest of

the polymer up to the breaking point. Once the polymer chain breaks, the cohesive stress will drop to zero and complete debonding occurs. For example, in the displacement-controlled experiments, the stress-strain curve may drop vertically to zero at a real critical interface opening displacement $[u_r]_{cr}$. It should be mentioned that in this process, the covalent bond force dominates the interaction mechanism of the interface over the van der Waals force. $[u_r]_{cr}^2$ acts as a transition point between the softening zone and the second hardening zone. With the increase of the density of chemical bonds, the softening zone becomes shorter, while the second hardening zone gets longer.

A MICROMECHANICS MODEL WITH CNT/MATRIX INTERFACE EFFECT

For simplicity, we consider a linear elastic polyethylene matrix reinforced with dispersed CNTs that are aligned and straight fibers, with identical radius, R, and infinite length. The fiber volume fraction is denoted by f.

Representative Volume Element (RVE)

The macroscopic stress, $\bar{\sigma}$, and strain, $\bar{\varepsilon}$, of the nanocomposite represent the collective, homogenized behavior of fibers and matrix. They are distinguished from the microscopic stress, σ, and strain, ε, in fibers and matrix, which are nonuniform due to the material inhomogeneities and satisfy their own constitutive laws, respectively,

$$\varepsilon^m = \mathbf{M}^m{:}\sigma^m, \varepsilon^f = \mathbf{M}^f{:}\sigma^f, \tag{9}$$

where the superscripts "f" and "m" represent the fiber and polymer matrix, and M is the compliance tensor matrix. To determine the constitutive relation between stress, $\bar{\sigma}$, and strain, $\bar{\varepsilon}$, for the composites, choose a representative volume element (RVE) consisting of nanotubes, matrix, and nanotube/matrix interfaces. The volume of the RVE is V, composed of matrix volume V^m and CNT volume V^f, and the volume fraction of fiber is defined as $f = \frac{V^f}{V^f+V^m}$. Considering the interface effect, the macroscopic stress, $\bar{\sigma}$, and strain, $\bar{\varepsilon}$, of the composites can be determined by the average theorem [37,38], as

$$\bar{\sigma} = f\sigma^f + (1-f)\sigma^m \tag{10}$$

$$\bar{\varepsilon} = f\varepsilon^f + (1-f)\varepsilon^m + f\varepsilon^{\text{int}}. \tag{11}$$

The additional term $f\boldsymbol{\varepsilon}^{\text{int}}$ in Eq. (11) accounts for the CNT/matrix interface effect, which is related to the displacement discontinuity

(jump) $[\mathbf{u}] = \mathbf{u}^m - \mathbf{u}^f$ across the CNT/matrix interface S^{int} and expressed as

$$\varepsilon^{\text{int}} = \frac{1}{2Vf} \int_{S^{\text{int}}} ([\mathbf{u}] \otimes \mathbf{n} + \mathbf{n} \otimes [\mathbf{u}]) dA, \tag{12}$$

where $\mathbf{u}^m$ and $\mathbf{u}^f$ are the displacements at the interface from the matrix and CNT side, respectively, and $\mathbf{n}$ is the unit normal vector on the interface pointing into the matrix.

The macroscopic strain, $\bar{\varepsilon}$, of the composite can be obtained in terms of the macroscopic stress, $\bar{\sigma}$, *via* Eqs. (9)–(11) as

$$\bar{\varepsilon} = \mathbf{M}^m : \bar{\sigma} + f\{(\mathbf{M}^f - \mathbf{M}^m) : \sigma^f + \varepsilon^{\text{int}}\}, \tag{13}$$

where ε^{int} and σ^f are to be determined from the interface cohesive law. For a simple case of isotropic matrix containing randomly distributed, long, and isotropic fibers subjected to a hydrostatic tension $\bar{\sigma}\mathbf{I}$ ($\boldsymbol{I}$ is the second-order identity tensor), the macroscopic strain of the composite is $\bar{\varepsilon}\mathbf{I}$, and $\bar{\varepsilon}$ is obtained from Eq. (13) as

$$\bar{\varepsilon} = \frac{1}{3K_m}\bar{\sigma} + \frac{f}{3}\left[\left(\frac{1}{3K_f} - \frac{1}{3K_m}\right)\sigma_{kk}^f + \varepsilon_{kk}^{\text{int}}\right], \tag{14}$$

where K_m and K_f are the elastic bulk moduli of the matrix and fibers, respectively, and $\varepsilon_{kk}^{\text{int}}$ is related to the displacement jump $[u_r]$ in the normal direction across the fiber/matrix interface *via* (12) by

$$\varepsilon_{kk}^{\text{int}} = 2\frac{[u_r]}{R}. \tag{15}$$

For perfectly bonded interfaces, *i.e.*, without any debonding, $\varepsilon_{kk}^{\text{int}} = 0$ and the average stress in the fiber σ_{kk}^f is the only parameter to be determined in terms of $\bar{\sigma}$ (or $\bar{\varepsilon}$). Accounting for the interface effect, a micromechanics model will be used to determine σ_{kk}^f and $\varepsilon_{kk}^{\text{int}}$ in terms of $\bar{\sigma}$. In conjunction with the cohesive law $\sigma^{\text{int}} = \sigma^{\text{int}}([u_r])$ in Eq. (2), Eq. (14) then gives the nonlinear stress-strain relation.

Dilute Model

Since the volume fraction of CNTs in the nanocomposites is usually low, a dilute model, which neglects the interactions among CNTs and is suitable for composites with low fiber/particle volume fraction, will be used to determine σ_{kk}^f and $\varepsilon_{kk}^{\text{int}}$ in terms of $\bar{\sigma}$. This model assumes that each infinite CNT with interface is embedded in an infinite pristine matrix subjected to a hydrostatic tension $\bar{\sigma}\mathbf{I}$. A cylindrical coordinate system (r, θ, z) is used to describe the problem, and $\bar{\sigma}$, $\bar{\varepsilon}$, and

σ^{int} denote the macroscopic stress and strain of the composite and the normal cohesive stress at the fiber/matrix interface, respectively. For the problem under this loading condition, the stresses in the fiber and the matrix take the following form [39]:

$$\sigma_{rr} = 2C + \frac{A}{r^2},\ \sigma_{\theta\theta} = 2C - \frac{A}{r^2},\ \sigma_{r\theta} = 0. \tag{16}$$

The unknowns C and A can be determined for both CNT and matrix according to the regularity condition at r = 0, the remote boundary condition $\sigma^m_{rr} = \bar{\sigma}$ at $r \to \infty$ and interface condition $\sigma^m_{rr} = \sigma^f_{rr} = \sigma^{\text{int}}$ at $r = R$. Since the fibers are assumed to be very long, the stress in the fiber direction for both fiber and matrix is given by the Reuss approximation [40],

$$\sigma^f_{zz} = \sigma^m_{zz} = \bar{\sigma}. \tag{17}$$

It should be mentioned that the Reuss approximation gives a lower bound solution and underestimates the reinforcing effect of fibers. Based on the determined stress fields in the fiber and the matrix, the radial displacement discontinuity (jump) across the fiber/matrix interface is expressed as

$$[u_r] = \frac{R}{E_m}\left[(2-\nu_m)\bar{\sigma} - (1+\nu_m)\sigma^{\text{int}}\right] - \frac{R}{E_f}\left[(1-\nu_f)\sigma^{\text{int}} - \nu_f\bar{\sigma}\right], \tag{18}$$

where E_f and ν_f are Young's modulus and Poisson's ratio of the fiber, respectively. The average stress in the fiber is $\sigma^f_{kk} = 2\sigma^{\text{int}} + \bar{\sigma}$, and together with Eqs. (14), (15), and (18) give the macroscopic stress and strain of nanocomposites in terms of the radial displacement jump $[u_r]$ across the fiber/matrix interface as

$$\bar{\sigma} = \frac{\frac{[u_r]}{R} + \left(\frac{1+\upsilon_m}{E_m} + \frac{1-\nu_f}{E_f}\right)\sigma^{\text{int}}([u_r])}{\frac{2-\nu_m}{E_m} + \frac{\nu_f}{E_f}} \tag{19}$$

$$\bar{\varepsilon} = \frac{1}{3K_m}\bar{\sigma} + \frac{f}{3}\left[\left(\frac{1}{3K_f} - \frac{1}{3K_m}\right)\left(2\sigma^{\text{int}}([u_r]) + \bar{\sigma}\right) + 2\frac{[u_r]}{R}\right]. \tag{20}$$

These two equations provide the nonlinear stress-strain relation of the CNT-reinforced composite.

Since the CNT Young's modulus, E_f, or the modulus of the effective fiber for a solid rod model in nanocomposites are much higher than that of the polymer matrix, E_m, Eqs. (19) and (20) can be simplified as

$$\bar{\sigma} = \frac{E_m}{2-\nu_m}\frac{[u_r]}{R} + \frac{1+\nu_m}{2-\nu_m}\sigma^{\text{int}}([u_r]) \tag{21}$$

$$\bar{\varepsilon} = \frac{1 - 2\nu_m + f}{2 - \nu_m}\frac{[u_r]}{R} + \frac{1}{E_m}\left[1 + \nu_m - \frac{f}{3}(5 - \nu_m)\right]\frac{1 - 2\nu_m}{2 - \nu_m}\sigma^{\text{int}}([u_r]) \quad (22)$$

These two simplified equations will be used to determine the constitutive relation of the CNT-reinforced composites, which are independent of the CNT Young's modulus.

STRESS-STRAIN RELATION FOR CNT-REINFORCED COMPOSITE

To study the effect of the interface cohesive law on CNT-reinforced composite, we revisit the problem studied by Tan *et al*. [29] where the composite is subject to a hydrostatic tension. Figure 3 shows the stress-strain curve for the composites reinforced with armchair (18, 18) CNTs (radius $R = 1.25\,nm$), in which the stress-strain curve of the pure polyethylene matrix is also provided for comparison. In this simulation, the CNT volume fraction is $f = 5\%$ and the chemical bond density is $\rho = 2\%$. A similar phenomenon as in [29] is observed. The stress-strain curve is almost straight and is above the straight line for the polymer matrix when the strain is less than a specific value (14.8% for example). Once the strain reaches 14.8% and the stress

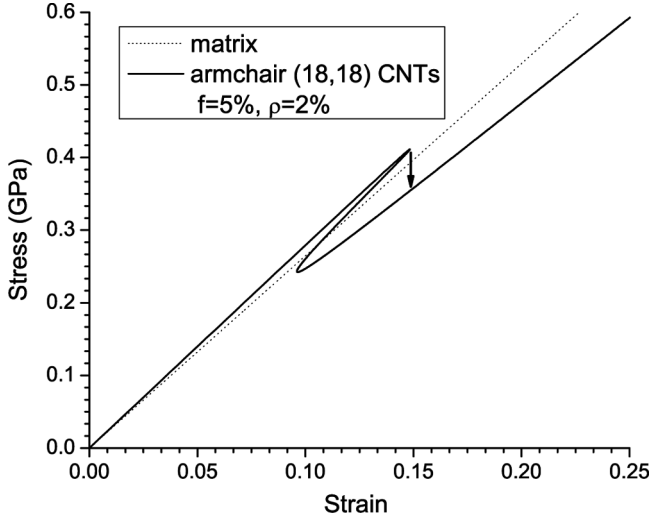

FIGURE 3 The stress-strain relationship of a CNT-reinforced polyethylene matrix composite and a pure polyethylene matrix subjected to hydrostatic tension.

reaches the peak value 411 MPa, both stress and strain start to decrease due to the interface softening behavior displayed in Fig. 2. The stress and strain start to increase again when the strain and the stress drop to 9.8% and 242 MPa. However, the stress-strain curve for the composite is lower than the straight line for the matrix, reflecting the weakening of the matrix. For the case studied in [29] where no chemical bonds are involved, this weakening is caused by the complete debonding between CNTs and matrix, which are equivalent to voids. The weakening demonstrated in Fig. 3 is still caused by the interface softening behavior, but not the interface debonding. It is anticipated the reinforcement of CNTs may occur again if the softening behavior is dominant over the hardening behavior of the interface with the increase of chemical bond density. For example, if the softening zone before the transition point $[u_r]^2_{cr}$ shown in Fig. 2 is much shorter, the reinforcement of the matrix may occur again. Within the deformation range and chemical bond density considered in the current work, even at relatively large strain, the interfacial hardening behavior can not suppress the weakening effect for the matrix caused by the previous interface softening. For composite subjected to displacement-controlled loading, the softening process will become dynamic, *i.e.*, the stress-strain curve may bypass the unloading stage and drop vertically from 411 to 353 MPa at the strain of 14.8% as illustrated by the arrow in Fig. 3, and then gradually increase.

Figure 4 shows the CNT size effect on the stress-strain curve with CNT volume fraction and chemical bond density being fixed at $f = 5\%$, $\rho = 1\%$. Before the first peak strength is reached, the bulk moduli of the composite reinforced with different sizes of CNTs are very similar. However, with the decrease of CNT radius from $R = 1.25$ *nm* [armchair (18, 18)], to 0.83 *nm* [armchair (12, 12)] and 0.42 *nm* [armchair (6, 6)], the peak strength increases from 408 to 421 and 464 MPa, respectively. Meanwhile, the critical strain associated with the peak strength also increases from 14.7 to 15.3 and 17.2%. It is clearly indicated in this figure that small CNTs give stronger reinforcement than large CNTs due to more interface areas between small CNTs and matrix at fixed volume fraction. Even after the interface softening takes effect, smaller CNTs are still more effective than larger CNTs as evidenced by the stress-strain curve for armchair (6, 6) being above the others. The volume fraction effect upon the macroscopic behavior of composite is plotted in Fig. 5 when the polyethylene matrix is reinforced with armchair (18, 18) CNTs. The chemical bond density is fixed at $\rho = 1\%$. When the volume fraction increases from $f = 1$ to 2 and 5%, the initial bulk modulus increases with the stress-strain curve for

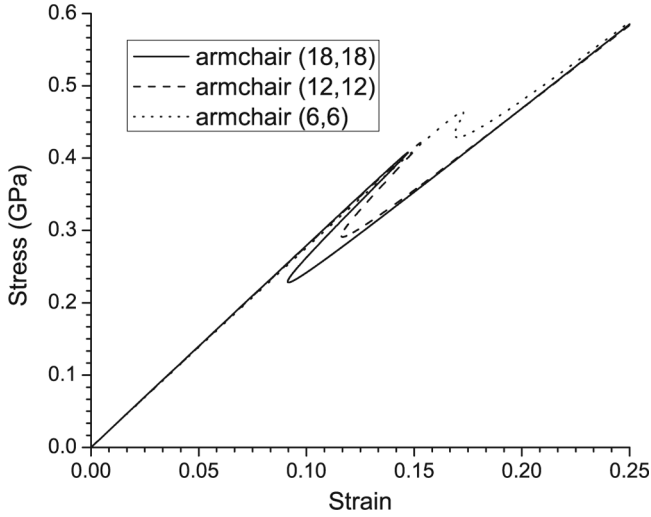

FIGURE 4 The CNT size effect on the macroscopic stress-strain relationship of a CNT-reinforced polyethylene matrix composite.

$f = 5\%$ being higher than for the other two cases. Once the softening behavior of the interface is in effect, the incremental bulk modulus decreases as expected. The peak strengths for different f are found

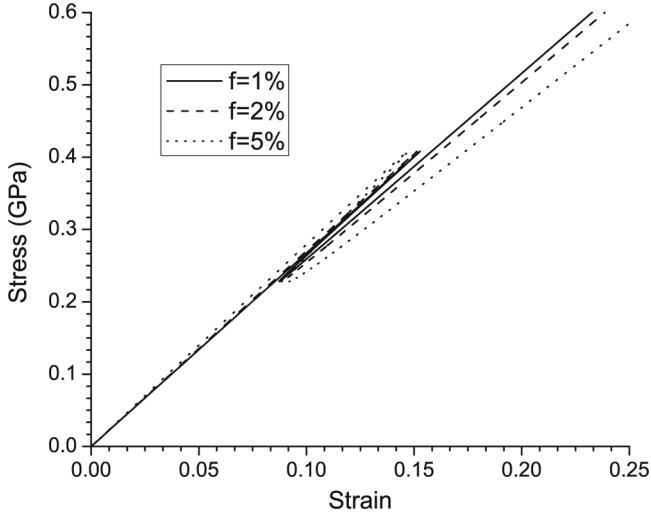

FIGURE 5 The effect of volume fraction of CNTs on the macroscopic stress-strain relationship of a CNT-reinforced polyethylene matrix composite.

to be exactly the same, *i.e.*, 408 MPa, which means that the CNT volume fraction has no effect on the composite strength as predicted in [29]. However, the critical strain associated with the peak strength has slight change from 15.2% for $f = 1\%$, to 15.1% for $f = 2\%$ and 14.7% for $f = 5\%$.

It is indicated in [34] that the interface bonding increases with the increase of chemical bond density. The interface bonding is governed by the total cohesive energy for the interface, which is the area under $\sigma^{\text{int}} \sim [\,u_r]$ curves in Fig. 2. It is seen from Fig. 2 the that when the interface opening is small, this cohesive energy is mainly controlled by the van der Waals force, while lower case with the increase of interface opening displacement, interface hardening reoccurs, resulting in the increase of cohesive energy and the improvement of the interface bonding. This interface behavior indicates that the stronger adhesion between CNTs and matrix caused by the chemical covalent bonds may significantly contribute to improve the mechanical behavior of CNT-reinforced composite only at relatively large deformation. Figure 6 shows the effect of chemical bond density on the stress-strain relationship of composite reinforced with armchair (18, 18) CNTs when the CNT volume fraction is fixed at $f = 5\%$. The initial bulk moduli are almost identical for all the cases before the peak strength is reached since this process is governed mainly by the van der Waals force. It

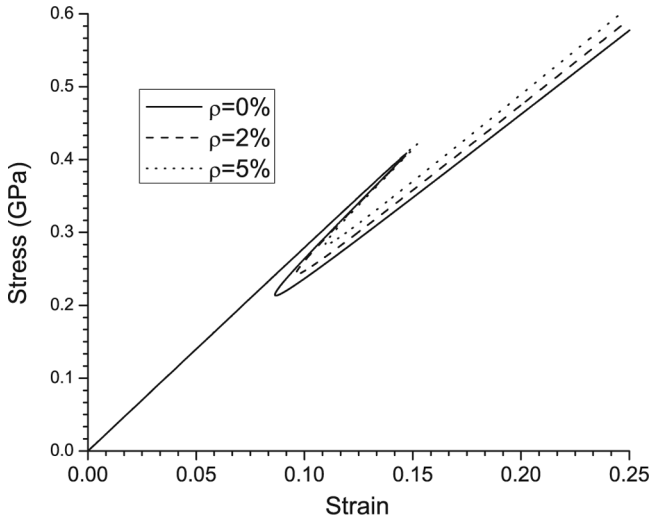

FIGURE 6 The effect of chemical bond density on the macroscopic stress-strain relationship of a CNT-reinforced polyethylene matrix composite.

is also observed in this figure that the composite strength (the peak strength) has slightly increased from 406 to 411 and 422 MPa when the chemical bond density changes from $\rho = 0$ to 2 and 5%. The corresponding strain for the peak strength also increases from 14.6 to 14.8 and 15.2%. With the increase of deformation, the stronger interface bonding contributes to improve the incremental modulus, *i.e.*, the stress-strain curve for $\rho = 5\%$ is higher than those for $\rho = 0\%$ and $\rho = 2\%$ at relatively large strain. It should be mentioned that for an interface with chemical bonds, the interfacial cohesion behavior has been changed in comparison with the interface without chemical bonds, *i.e.*, interface hardening is present again when the interface opening is beyond $[u_r]_{cr}^2$ for interfacial interaction involving chemical bonds, as shown in Fig. 2. However, it is also observed in Fig. 6 that chemical bonds do not affect the tendency of the overall stress-strain relationship for the composite. Therefore, it is concluded that the contribution of chemical bonds is to harden the interface at relatively large deformation, and thus, to improve the mechanical behavior of CNT composites.

CONCLUSIONS

The nonlinear cohesive law accounting for both van der Waals force and chemical covalent bonds is incorporated in the micromechanics model to study the macroscopic behavior of CNT-reinforced composite. With the increase of chemical bond density, the interface adhesion can be improved. Carbon nanotubes are found to improve the mechanical behavior of composite at small strain. However, the composite might be weakened at relatively large strain because of the softening behavior of the interface. Whether the improvement or weakening occurs depends on the density of chemical bonds. The increase of the interface adhesion between CNTs and polymer matrix caused by the chemical bonds may significantly improve the composite behavior only at relatively large strain. The improvement effect upon the composite strength and the corresponding critical strain is not significant for this opening deformation mode of the interface. Further atomistic study or experimental work may be needed to verify the predicted results in the current work for the macroscopic behavior of composites considering the effect of interfaces with opening deformation mode.

ACKNOWLEDGMENT

This work was supported by Natural Sciences and Engineering Research Council of Canada (NSERC).

REFERENCES

[1] Iijima, S., *Nature* **354**, 56–58 (1991).
[2] Thess, A., Lee, R., Nikolaev, P., Dai, H. J., Petit, P., Roert, J., Xu, C. H., Lee, Y. H., Kim, S. G., Rinzler, A. G., Colbert, D. T., Scuseria, G. E., Tomanek, D., Fischer, J. E., and Smalley, R. E., *Science* **273**, 483–487 (1996).
[3] Treacy, M. M. J., Ebbesen, T. W., and Gibson, J. M., *Nature* **381**, 678–680 (1996).
[4] Wong, E. W., Sheehan, P. E., and Lieber, C. M., *Science* **277**, 1971–1975 (1997).
[5] Yu, M. F., Files, B. S., Arepalli, S., and Ruoff, R. S., *Phys. Rev. Lett.* **84**, 5552–5555 (2000).
[6] Yu, M. F., Lourie, O., Dyer, M. J., Moloni, K., Kelly, T. F., and Ruoff, R. S., *Science* **287**, 637–640 (2000).
[7] Yakobson, B. I., Brabec, C. J., and Bernholc, J., *Phys. Rev. Lett.* **76**, 2511–2514 (1996).
[8] Popov, V. N., Van Doren, V. E., and Balkanski, M., *Phys. Rev. B* **61**, 3078–3084 (2000).
[9] Thostenson, E. T., Ren, Z. F., and Chou, T. W., *Compos. Sci. Technol.* **61**, 1899–1912 (2001).
[10] Thostenson, E. T., Li, C. Y., and Chou, T. W., *Compos. Sci. Technol.* **65**, 491–516 (2005).
[11] Maruyama, B. and Alam, K., *SAMPE J.* **38**, 59–68 (2002).
[12] Deepak, S., Wei, C., and Cho, K., *Appl. Mech. Rev.* **56**, 215–230 (2003).
[13] Harris, P. J. F., *Int. Mater. Rev.* **49**, 31–43 (2004).
[14] Ajayan, P. M., Schadler, L. S., Giannaris, C., and Rubio, A., *Adv. Mater.* **12**, 750–753 (2000).
[15] Qian, D. and Dickey, E. C., *J. Microsc.* **204**, 39–45 (2001).
[16] Schadler, L. S., Giannaris, S. C., and Ajayan, P. M., *Appl. Phys. Lett.* **73**, 3842–3844 (1998).
[17] Andrews, R., Jacques, D., Rao, A. M., Rantell, T., Derbyshire, F., Chen, Y., Chen, J., and Haddon, R. C., *Appl. Phys. Lett.* **75** (9), 1329–1331 (1999).
[18] Baughman, R. H., Zakhidov, A. A., and de Heerm, W. A., *Science* **297**, 787–792 (2002).
[19] Qian, D., Dickey, E. C., Andrews, R., and Rantell, T., *Appl. Phys. Lett.* **76**, 2868–2870 (2000).
[20] Lordi, Y. and Yao, N., *J. Mate. Research* **15**, 2770–2779 (2000).
[21] Wagnger, H. D., Lourie, O., Feldman, Y., and Tenne, R., *Appl. Phys. Lett.* **72**, 188–190 (1998).
[22] Frankland, S. J. V., Caglar, A., Brenner, D. W., and Griebel, M., *J. Phys. Chem. B* **106**, 3046–3048 (2002).
[23] Frankland, S. J. V., Harik, V. M., Odegard, G. M., Brenner, D. W., and Gates, T. S., *Compos. Sci. Technol.* **63**, 1655–1661 (2003).
[24] Gou, J., Minaie, B., Wang, B., Liang, Z., and Zhang, C., *Comput. Mater. Sci.* **31**, 225–236 (2004).
[25] Li, C. and Chou, T. W., *J. Nanosci. Nanotechnol.* **3**, 423–430 (2003).
[26] Liao, K. and Li, S., *Appl. Phys. Lett.* **79**, 4225–4227 (2001).
[27] Wagner, H. D., *Chem. Phys. Lett.* **361**, 57–61 (2002).
[28] Jiang, L. Y., Huang, Y. G., Jiang, H., Ravichandran, G., Gao, H., Hwang, K. C., and Liu, B., *J. Mech. Phys. Solids* **54**, 2436–2452 (2006).
[29] Tan, H., Jiang, L. Y., Huang, Y., Liu, B., and Kwang, K. C., *Compos. Sci. Technol.* **67**, 2941–2946 (2007).
[30] Velasco-Santos, C., Martinez-Hernandez, A. L., Fisher, F. T., Ruoff, R., and Castano, V. M., *Chem. Maters.* **15**, 4470–4475 (2003).

[31] Mylvaganam, K. and Zhang, L. C., *J. Phys. Chem. B* **108**, 5217–5220 (2004).
[32] McIntosh, D., Khabashesku, V. N., and Barrera, E. V., *Chem. Maters.* **18**, 4561–4569 (2006).
[33] Shofner, M. L., Khabashesku, V. N., and Barrera, E. V., *Chem. Maters.* **18**, 906–913 (2006).
[34] Jiang, L. Y., *Math. Mech. Solids*, in press.
[35] Brenner, D. W., Shenderova, O. A., Harrison, J. A., Stuart, S. J., Ni, B., and Sinnott, S. B., *J. Phys.-Condensed Matter* **14**, 783–802 (2002).
[36] Huang, Y., Wu, J., and Hwang, K. C., *Phys. Rev. B* **74**, 245413 (2006).
[37] Benveniste, Y., *Mech. Mater.* **6**, 147–157 (1987).
[38] Tan, H., Huang, Y., Liu, C., and Geubelle, P. H., *Int. J. Plasticity* **21**, 1890–1918 (2005).
[39] Lu, M. W. and Luo, X. F., *Theory of Elasticity* (Tsinghua University, Beijing 1990). 1st ed., Ch. 7, pp. 259–264.
[40] Reuss, A. Z., *Angew. Math. Mech.* **9**, 49–58 (1929).